ChemComm

Accepted Manuscript

This article can be cited before page numbers have been issued, to do this please use: B. Maji and J. Choudhury, *Chem. Commun.*, 2019, DOI: 10.1039/C9CC00972H.

ROYAL SOCIETY OF CHEMISTRY

rsc.li/chemcomm

View Article Online
DOI: 10.1039/C9CC00972H

Journal Name

COMMUNICATION

Switchable hydrogenation with betaine–derived bifunctional Ir–NHC catalyst†

Received 00th January 20xx,
Accepted 00th January 20xx

DOI: 10.1039/x0xx00000x

www.rsc.org/

Babulal Maji and Joyanta Choudhury*

A bifunctional iridium catalyst based on 'uracil–abnormal NHC' hybrid ligand platform was developed for switchable hydrogenation of quinoxalines. Control studies suggested heterolytic H_2 activation via metal-ligand bifunctional operation to generate Ir–H and an adjacent protic O–H group for facile H^+/H^- transfer to quinoxaline. Presence of base blocked the most essential H^+-transfer step thus switching off the catalysis, while acid stimulus reversed the action to switch on the reaction again.

Investigating the influence of external chemical or physical stimuli on the function of suitably designed homogeneous and heterogeneous catalysts creates knowledge that may contribute in developing new artificial switchable catalysts.[1] However, as far as catalyst design is concerned, it is always a challenging task to create a harmonious combination of the stimuli-triggered property switching and application-worthy smart catalytic response. Nevertheless, the field of artificial switchable catalysis blossomed exciting developments over the past few years with notable applications in several areas ranging from polymerization and organic synthesis, energy research to material science.[1] Alongside the most popular stimuli such as light, redox potential, pH, and metal-coordination, recently reversible alteration of reaction conditions was also utilized as stimulus to regulate the rate and/or selectivity of catalytic reactions.[1,2] To control such regulation, while the former stimuli modulate structural and/or stereoelectronic property of the catalyst itself, the later generally affects the reaction path and/or intermediates.

Our recent success on reversible and switchable hydrogenation/dehydrogenation catalysis was based on a strategy of applying acid/base-stimulated switchable metal-ligand coordination modes within the catalyst backbone to toggle the stereoelectronic property and thereby the activity of the catalysts.[3] Striving towards new switching strategy and pathway, herein we present a base-switchable hydrogenation reaction with a bifunctional Ir–N-heterocyclic carbene (NHC) catalyst. In the present work, atmospheric-pressure hydrogenation of quinoxalines was selected to demonstrate the switchable action of the catalyst. It is noteworthy to mention here that, at the forefront of alternative energy research, catalytic hydrogenation of liquid N-heteroarenes (such as quinolines, quinoxalines, naphthyridines etc.) received a renewed attention.[4] This is because hydrogenated N-heterocycles are proposed as suitable hydrogen storage/carrier systems, and interestingly fuel cells and flow batteries using such liquid organic hydrogen carriers (LOHCs) are being investigated as promising energy technology.[4,5]

The design of the new catalyst involved the use of a 'uracil–abnormal NHC' hybrid bidentate ligand bound to the Cp^*Ir^{III} catalytic center (Fig. 1A). The uracilate motif within the resulting Ir-betaine architecture present in the catalyst backbone is prone to lactam-lactim tautomerization[6] resulting in a pendent base (Ir–N=C–***O***$^-$) which can render metal-ligand bifunctionality[7] favorable for heterolytic H_2 activation (Fig. 1B). We hypothesize that such heterolytic H_2 activation would generate a coordinatively saturated catalytic intermediate consisting of **Ir–*H*** and Ir–N=C–***OH*** units (structure **IV**, (Fig. 1B), susceptible for consecutive H^+/H^- transfer to quinoxaline (**Q**) substrate via outer-sphere mechanism (Fig. 1C). It was reported earlier in several studies that hydride (H^-) transfer to protonated quinolines rather than to the free neutral quinolines is a feasible path in their hydrogenation.[4] Considering similar pathway for quinoxalines as well, we observed facile hydrogenation catalysis by using 1 mol% **Ir-U$_{NH}$** as catalyst under H_2 balloon atmosphere resulting in 90-96% yield of 1,2,3,4-tetrahydroquinoxalines in just 1.5 h at 50 °C in 2,2,2-trifluoroethanol (TFE)/H_2O (3:1, v/v) mixed solvent (Fig. 1C). Notably, a catalyst loading of 0.5 mol% or the reaction temperature of 30 °C were also effective albeit with a slightly lower rate. The hydrogenation protocol with this catalyst was also found to be applicable effectively for quinolines also (see ESI). It is known that TFE helps effective solvation and dissociation of the chloride ligand attached to the Ir^{III} center of

Organometallics & Smart Materials Laboratory, Department of Chemistry, Indian Institute of Science Education and Research (IISER) Bhopal, Bhopal 462 066, India. E-mail: joyanta@iiserb.ac.in.

† Electronic Supplementary Information (ESI) available: CCDC 1895154 (**Ir-U$_{NH}$**). See DOI: 10.1039/x0xx00000x

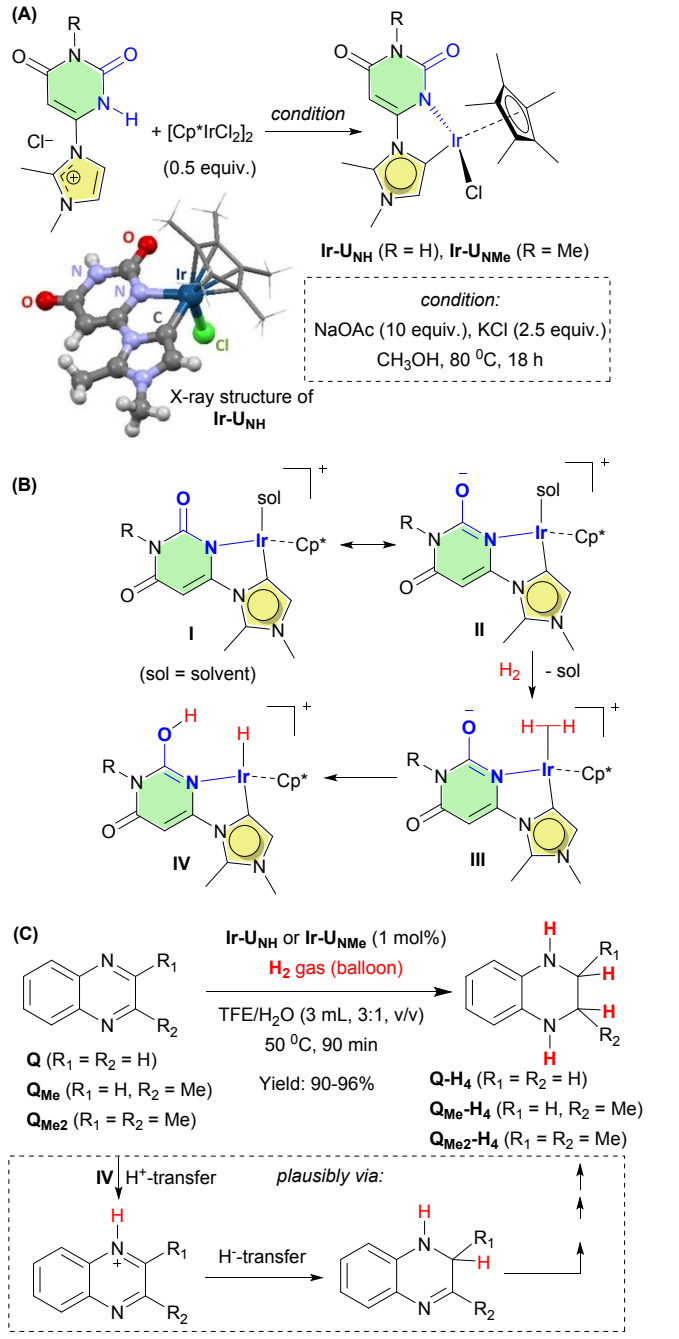

Fig. 1 (A) Synthetic scheme of the complexes **Ir-U$_{NH}$** and **Ir-U$_{NMe}$**, and crystal structure of **Ir-U$_{NH}$**; (B) plausible lactam-lactim tautomerization for the complex backbone, and proposed bifunctional heterolytic H_2-activation. *The possible second -N(H)-C(=O)- ↔ -N=C(OH)- tautomerization for complex* **Ir-U$_{NH}$** *was not shown;* (C) general scheme for catalytic hydrogenation of quinoxalines, and proposed H^+/H^- transfer pathway.

the catalyst,[4f] thus creating the vacant site required for facile H_2-coordination, followed by subsequent catalytic steps. Next, a time profile of the catalysis with quinoxaline as substrate and **Ir-U$_{NH}$** (1 mol%) as catalyst in TFE/H_2O solvent mixture was derived, showing smooth formation of the hydrogenated product during the course of the reaction (Fig. 2A). Even, the catalysis in the absence of TFE, i.e., only in H_2O as solvent was also successful. Interestingly, the catalysis was found to be almost switched off (product yield of only 6% in 1.5 h) when

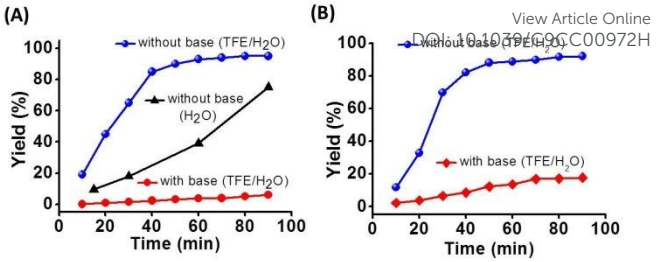

Fig. 2 Catalytic hydrogenation of quinoxaline (Q) with (A) **Ir-U$_{NH}$** and (B) **Ir-U$_{NMe}$** as catalyst in the absence (blue trace) and presence (red trace) of base (K_2CO_3).

the reaction was performed in the presence of 40 mol% K_2CO_3 under otherwise identical conditions (Fig. 2A). This result was remarkable and to verify if this was due to the presence of the acidic N–H group within the uracilate backbone of the catalyst **Ir-U$_{NH}$**, control catalytic reactions were performed with the N–Me version **Ir-U$_{NMe}$**. The results were found to be similar; i.e., the highly efficient reaction observed with **Ir-U$_{NMe}$** was almost switched off (product yield of 17% in 1.5 h) in the presence of base (K_2CO_3) (Fig. 2B).

Next, the feasibility of the most vital switchable action of the catalyst **Ir-U$_{NH}$** (1 mol%) for the hydrogenation of quinoxaline was tested by applying base (K_2CO_3) to switch off and the reverse stimulus, i.e., an acid (HCl) to switch it on again. Thus an ongoing catalytic reaction could be consecutively switched off and on for multiple times with these stimuli (Fig. 3A). Although, the probable buffering effect due to salt formation during consecutive addition of K_2CO_3 and HCl did not hamper

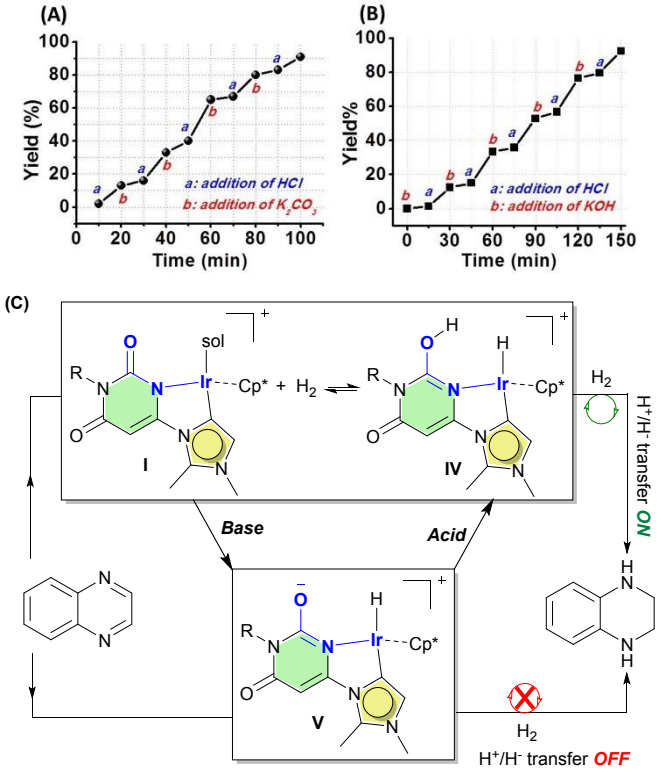

Fig. 3 (A) and (B) Switchable hydrogenation of quinoxaline (**Q**) with **Ir-U$_{NH}$** as catalyst; (C) the working proposal for the switchable action of the catalyst.

View Article Online
DOI: 10.1039/C9CC00972H

the activity much at the later stage of the catalysis, the switching experiment was performed using KOH and HCl as stimuli. Delightedly, the resulting OFF/ON switching kinetics was found to be improved (Fig. 3B). Based on these results, a working mechanism has been proposed to explain the observed switchability in this case (Fig. 3C). Of course, other proposals can also be put forth which can not be ruled out at this moment without extensive mechanistic investigation including computational studies. However, to gain insight into the hypothesis on bifunctional H_2 activation and switchable hydrogenation as shown in Figs. 1B,C and 3C, few control ^{1}H NMR spectroscopic studies were performed. The results of these investigations have been described below.

First of all, a solution of complex **Ir-U$_{NH}$** (5.2 µmol) was made in 0.5 mL of CD_3CN containing 50 µL of TFE and 20 µL of H_2O. The ambient temperature ^{1}H NMR spectrum of this light yellow-colored solution was consistent with the characteristic resonances of all the H's of **Ir-U$_{NH}$** (Fig. 4A-a and ESI). However, the N–***H*** (or the O–***H***) resonance was not observed, probably due to fast tautomerization in the present solvent mixture. When this solution was exposed to H_2 gas for few minutes, the color changed to red, and in the ^{1}H NMR spectrum the characteristic iridium-hydride (Ir–***H***) peak was observed at −14.65 ppm (Fig. 4A-b). This was associated with the appearance of an additional new set of peaks (with expected integration ratio corresponding to the ligand backbone), plausibly due to the intermediate **IV** generated by the heterolytic cleavage of H_2. Interestingly, the evolution of a broad singlet peak at ~9.17 ppm (having integration of one H to the abovementioned backbone protons) was suggestive and indicative toward the presence of an Ir–N=C–***OH*** proton. Similar NHC-Ir^{III}(Cp*)-pyridinol complexes, reported by Papish and co-workers exhibited the O–***H*** resonances at 10.3 ppm in CD_3CN.[8] Notably, the conversion to this hydride intermediate complex from the parent **Ir-U$_{NH}$** was found to be ~15%. The rest of complex **Ir-U$_{NH}$** was also present in the same solution as evident from the spectrum with the corresponding backbone protons having desired integration ratio, along with the appearance of the earlier-obscured lactim O–***H*** at ~9.51 ppm. The reason of this unexpected behaviour is not clear to us at this moment, and needs more extensive investigation. Nevertheless, when quinoxaline (**Q**) (5.1 µmol) was added to this mixture in presence of H_2 gas, the proposed hydride species disappeared along with its resonances including the peaks at −14.65 ppm (for hydride Ir–***H***) and at ~9.17 ppm (for proton O–***H***) (Fig. 4A-c). The color of the solution also changed back to yellow. Additionally, ~15% of the hydrogenated product 1,2,3,4-tetrahydroquinoxaline (**Q-H$_4$**) was formed as evident from its characteristic multiplet peaks at ~6.46-6.49 ppm. This fact suggested that only ~15% quinoxaline reacted with the available ~15% hydride species via H^+/H^- transfer twice in presence of H_2 gas to produce the hydrogenated product in ~15% yield. On the contrary, a similar ^{1}H NMR spectroscopic study, as discussed above, with catalyst **Ir-U$_{NH}$** but now in the presence of base (K_2CO_3) showed the generation of Ir–***H*** but no Ir–N=C–***OH*** upon reaction with H_2 gas (Fig. 4B-b). The base would have captured the acidic H^+

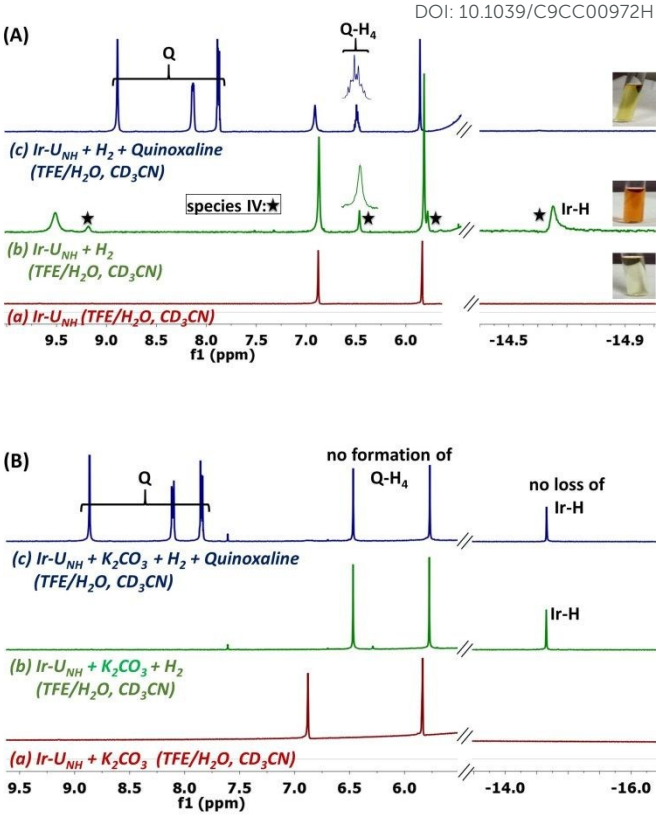

Fig. 4 (A) ^{1}H NMR spectroscopic monitoring for the reaction of **Ir-U$_{NH}$** catalyst with H_2 gas followed by addition of quinoxaline (**Q**) leading to the formation of hydrogenated quinoxaline (**Q-H$_4$**); the images of the corresponding solutions were shown alongside; (B) ^{1}H NMR spectroscopic monitoring for the reaction of **Ir-U$_{NH}$** catalyst with H_2 gas in the presence of base (K_2CO_3) followed by addition of quinoxaline (**Q**) showing no consumption of iridium hydride and no product formation.

available from heterolytic cleavage of H_2. Under such circumstances, when quinoxaline was added to the reaction mixture, the characteristic Ir–***H*** peak at −14.65 ppm did not disappear and no hydrogenation occurred (Fig. 4B-c). This switching off of the reaction could be due to the lack of initial H^+ transfer to quinoxaline to produce protonated quinoxaline which could accept the available hydride from the Ir–H species. Hydride transfer was not feasible to the free neutral quinoxaline, thus disfavoring hydrogenation. This off condition could be switched on again by adding acid (HCl) to the reaction mixture leading to the formation of the hydrogenated product 1,2,3,4-tetrahydroquinoxaline (**Q-H$_4$**). Finally, the catalytic hydrogenation of quinoxaline with **Ir-U$_{NH}$** as catalyst using D_2 gas led to the incorporation of D atoms into the product, thus confirming that hydrogen gas was the source of hydrogen atom in this reaction (see SI).

In summary, a switchable hydrogenation protocol was demonstrated with a new bifunctional Ir–NHC catalyst. Under ambient H_2 pressure, the catalyst was highly active toward hydrogenation of quinoxalines to load two molecules of H_2 per molecule of the N-heteroarene. Action of a base stimulus to this catalysis led to switching off the hydrogenation, while a reverse stimulus, an acid switched it on again. Mechanistic hypothesis for the switching phenomenon was examined with

some control in situ NMR experiments, which suggested a bifunctional pendant base-assisted heterolytic H_2 activation to generate iridium hydride and an adjacent protic O–H functionality for facile H^+/H^- transfer to the substrate quinoxalines during hydrogenation. Presence of base modulated the mechanism and plausibly did not allow the ready availability of any protic O–H or proton to be transferred to quinoxaline, which itself was a bad substrate for accepting hydride from Ir–H. Interestingly, subsequent acid addition reverses the situation and triggered hydrogenation by protonating the neutral quinoxaline molecule to make it now susceptible for hydride transfer from Ir–H generated from H_2. These results exemplified the possibility of devising new switchable hydrogenation catalysis protocol by intercepting the mechanistic paths with a harmonious combination of suitable stimuli and appropriately designed catalyst. As the present catalyst was also found to be effective in dehydrogenation of the tetrahydroquinoxaline products (ESI), switchable and reversible dehydrogenation/hydrogenation catalysis would be the subject of future study.

This research was generously funded by SERB-DST, Govt. of India (grant no. EMR/2016/003002) and IISER Bhopal. B.M. thanks UGC, Govt. of India for doctoral fellowship. We thank Abhishek Kumar for his help.

Notes and references

1 For reviews, see: (*a*) J. Choudhury, *Tetrahedron Lett.*, 2018, **59**, 487–495; (*b*) J. Choudhury and S. Semwal, *Synlett*, 2018, **29**, 141–147; (*c*) V. Blanco, D.A. Leigh and V. Marcos, *Chem. Soc. Rev.*, 2015, **44**, 5341–5370; (*d*) B.M. Neilson and C.W. Bielawski, *ACS Catal.*, 2013, **3**, 1874–1885; (*e*) A.J. Teator, D.N. Lastovickova and C.W. Bielawski, *Chem. Rev.*, 2016, **116**, 1969–1992; (*f*) G. Romanazzi, L. Degennaro, P. Mastrorilli and R. Luisi, *ACS Catal.*, 2017, **7**, 4100–4114; (*g*) A.J. Teator and C.W.J. Bielawski, *Polym. Sci. Part A Polym. Chem.*, 2017, **55**, 2949–2960; (*h*) Z. Yu and S. Hecht, *Chem. Commun.*, 2016, **52**, 6639–6653; (*i*) S.M. Guillaume, E. Kirillov, Y. Sarazin and J.-F. Carpentier, *Chem. Eur. J.*, 2015, **21**, 7988–8003; (*j*) F. Wang, X. Liu and I. Willner, *Angew. Chem. Int. Ed.*, 2015, **54**, 1098–1129; (k) M. Schmittel, *Chem. Commun.*, 2015, **51**, 14956–14968; (*l*) A.M. Lifschitz, M.S. Rosen, C.M. McGuirk and C.A. Mirkin, *J. Am. Chem. Soc.*, 2015, **137**, 7252–7261; (*m*) R. Göstl, A. Senf and S. Hecht, *Chem. Soc. Rev.*, 2014, **43**, 1982–1996; (*n*) F.A. Leibfarth, K.M. Mattson, B.P. Fors, H.A. Collins, C.J. Hawker, *Angew. Chem. Int. Ed.*, 2013, **52**, 199–210; (*o*) N. Kumagai and M. Shibasaki, *Catal. Sci. Technol.*, 2013, **3**, 41-57. (*p*) R.S. Stoll and S. Hecht, *Angew. Chem. Int. Ed.*, 2010, **49**, 5054–5075; (*q*) U. Lüning, *Angew. Chem. Int. Ed.*, 2012, **51**, 8163–8165.

2 (*a*) C. Hu, R. Duan, S. Yang, X. Pang and X. Chen, *Macromolecules*, 2018, **51**, 4699−4704; (*b*) O. Coulembier, S. Moins, R. Todd and P. Dubois, *Macromolecules*, 2014, **47**, 486−491.

3 (*a*) S. Semwal and J. Choudhury, *ACS Catal.*, 2016, **6**, 2424–2428; (*b*) S. Semwal and J. Choudhury, *Angew. Chem. Int. Ed.*, 2017, **56**, 5556–5560; (*c*) S. Semwal, A. Kumar and J. Choudhury, *Catal. Sci. Technol.*, 2018, **8**, 6137-6142.

4 For selected recent examples, see: (*a*) G. E. Dobereiner, A. Nova, N. D. Schley, N. Hazari, S. J. Miller, O. Eisenstein and R. H. Crabtree, *J. Am. Chem. Soc.*, 2011, **133**, 7547–7562; (*b*) K. Fujita, Y. Tanaka, M. Kobayashi and R. Yamaguchi, *J. Am. Chem. Soc.*, 2014, **136**, 4829−4832; (*c*) C. Wang and J. Xiao, *Chem. Commun.*, 2017, **53**, 3399-3411; (*d*) Á. Vivancos, M. Beller and M. Albrecht, *ACS Catal.*, 2018, **8**, 17–21; (e) Z-J. Yao,, N. Lin, X-C. Qiao, J-W. Zhu and W. Deng, *Organometallics*, 2018, **37**, 3883−3892; (*f*) J. Wu, J. H. Barnard, Y. Zhang, D. Talwar, C. M. Robertson and J. Xiao, *Chem. Commun.*, 2013, **49**, 7052-7054; (g) H. Zhou, Z. Li, Z. Wang, T. Wang, L. Xu, Y. He, Q-H. Fan, J. Pan, L. Gu and A. S. C. Chan, *Angew. Chem. Int. Ed.*, 2008, **47**, 8464 –8467.

5 (*a*) P. Preuster, C. Papp and P. Wasserscheid, *Acc. Chem. Res.*, 2017, **50**, 74–85; (*b*) M. Markiewicz, Y-Q. Zhang, M. T. Empl, M. Lykaki, J. Tho¨ming, P. Steinberg and S. Stolte, *Energy Environ. Sci.*, 2019, **12**, 366--383; (*c*) R. H. Crabtree, *ACS Sustainable Chem. Eng.*, 2017, **5**, 4491−4498; (d) K. Müller, K. Brooks and T. Autrey, *Energy Fuels*, 2018, **32**, 10008−10015.

6 (*a*) M. Yamada and I. Honma, *ChemPhysChem*, 2004, **5**, 724-728; (*b*) C. S. Peng and A. Tokmakoff, *J. Phys. Chem. Lett.*, 2012, **3**, 3302−3306; (c) Y. Nakane, T. Takeda, N. Hoshino, K. Sakai and T. Akutagawa, *J. Phys. Chem. A*, 2015, **119**, 6223−6231; (d) C. S. Peng, C. R. Baiz and A. Tokmakoff, *Proc. Natl. Acad. Sci. U.S.A*., 2013, **110**, 9243-9248; (e) J. Zhang, N. Pidlypnyi, M. Nieger, J. C. Namysloa and A. Schmidt, *Org. Biomol. Chem.*, 2014, **12**, 2737–2744.

7 For selected reviews, see: (*a*) S. Kuwata and T. Ikariya, *Chem. Commun.*, 2014, **50**, 14290—14300; (*b*) R. H. Morris, *Acc. Chem. Res.,* 2015, **48**, 1494−1502; (*c*) J. R. Khusnutdinova and D. Milstein, *Angew. Chem. Int. Ed.*, 2015, **54**, 12236–12273; (*d*) L. V. A. Hale and N. K. Szymczak, *ACS Catal.*, 2018, **8**, 6446−6461.

8 S. Siek, D. B. Burks, D. L. Gerlach, G. Liang, J. M. Tesh, C. R. Thompson, F. Qu, J. E. Shankwitz, R. M. Vasquez, N. Chambers, G. J. Szulczewski, D. B. Grotjahn, C. E. Webster and E. T. Papish, Organometallics, 2017, **36**, 1091−1106.